Water in keratin

Piezoelectric, dielectric, and elastic experiments

Hideatsu Maeda
Research Institute for Polymers and Textiles, Tsukuba, Ibaraki, 305 Japan

ABSTRACT To investigate actions of water in keratin, the piezoelectric, dielectric, and elastic constants are measured at 10 Hz, at temperatures between −160 and 150°C, and at various hydration levels.

From changes in the piezoelectric, dielectric, and dynamic mechanical parameters with moisture content (m.c.), we have identified three regimes (I, II, and III) in the hydration of water for keratin.

At high hydration (21% m.c.) around 0°C, the piezoelectric constants for keratin steeply decrease with increasing temperature. This may be attributed to interfacial polarization which is strongly related to self-associated water molecules (particularly regime III water) just around crystalline helical regions which can exhibit the stress-induced, i.e., piezoelectric, polarization and may be attributed to electrode polarization induced by the increase of mobile ions in the amorphous matrix region, some of which would be released from their trapped states just around the piezoelectric phase by the regime III water.

With increasing hydration, the elastic constants for keratin are found to increase below −70°C and decrease above −70°C. This suggests a viscoelastic transition of the keratin structure due to bound water (regime II water).

The piezoelectric, dielectric, and elastic loss peaks are found at around −120°C for hydrated keratin, believed to be due to tightly bound water (regime I water), which acts only to stiffen the keratin structure.

The adsorption regions of water in keratin are discussed by a piezoelectric two-phase model, which consists of piezoelectric and nonpiezoelectric phases. It is proposed that water molecule would at least adsorb in the nonpiezoelectric phase.

INTRODUCTION

Keratin has been shown to have a composite structure in which filaments or microfibrils are embedded in a ground substance or matrix. The microfibrils are ~72–76 Å in diameter and spaced ~86.5–97.5 Å apart (1). X-Ray analysis and electron microscopy have demonstrated the existence of an axial repeat of 200 Å in the microfibrils (2). The microfibrils further have been indicated to have a helical symmetry by low angle x-ray diffractions (3). The major constituent of the microfibrils is believed to be low-sulfur proteins. The matrix is considered to be less ordered and at least globular in nature. The constituent is believed to be high-sulfur proteins (4).

The interaction of water with keratin has been extensively investigated by many.

King (5) and Algie (6) found that the increase of the dielectric constants of hydrated wool is due not only to adsorbed water but also protein itself. Algie et al. (7) further found dielectric loss peaks due to water for wool, and discussed the molecular mechanism of the dielectric relaxation.

Algie (8) and Algie and Watt (9) studied the effect of changes in the relative humidity on the electrical conductivity of wool fibers and found that the variation of conductance can be considered in three stages corresponding to three ranges of water content.

The elastic properties of hydrated keratin were investigated with the tortional measurements. Speakman (10) and Druhala and Feughelman (11) measured hydration and temperture dependence of the rigidity of keratin to discuss actions of water in it. Menefee and Yee (12) found an elastic loss peak due to water molecules in wool.

Fukada et al. (13) measured the piezoelectric constants of horn keratin and found that they are greatly influenced by water.

Lynch and Marsden (14, 15) investigated the mobility of water molecules in keratin by NMR spectroscopies, and they supported a five-phase model of bound water proposed by Feughelman and Haly (16).

Feughelman (17) first proposed a two-phase model of keratin to explain the mechanical behavior, such as swelling and tortional properties. Further, Feughelman and Haly proposed a series-zone model (18) accounting for the postyield region of the load-extension curve, and afterwards Feughelman (19) improved the model by using an x-ray model for the microfibril proposed by Fraser et al. (2).

Possible adsorption regions of water molecules in keratin are proposed from x-ray diffraction studies by Heidemann and Halboth (20), Fraser et al. (2), and Spei and Zanh (21, 22), but two different regions for water adsorp-

0006-3495/89/11/861/08 $2.00

tion are proposed, one is amorphous matrix and the other is microfibrils.

The main purpose of the present paper is to systematically reexamine adsorption sites of water and their actions in keratin by use of piezoelectric, dielectric, and elastic measurements. It should be noted that elastic and dielectric measurements can provide averaged mechanical and electric properties of specimens as a whole, but the piezoelectric measurements can separately provide the electromechanical information about the crystalline regions and about the amorphous regions surrounding them. We consider that the piezoelectric polarization can be induced by a deformation of uniaxially aligned α-helical portions in the microfibril. Thus, we hoped to get some information on the adsorption sites for water in keratin.

MATERIALS AND METHOD

Calf horn was used as keratinous substance in the present investigation. The typical dimensions of the samples for piezoelectric and dielectric measurements were 15 × 10 × 0.5 mm. The direction of the long side of the samples is at 45° to the orientation axis of keratin fibers so as to measure the piezoelectric coefficients d_{14} and e_{14}, which are the coupling between a polarization Px in the x-direction and a shear stress and strain Tyz in the yz-plane respectively, as shown in Fig. 1. (For simplicity, the subscript 14 and negative sign of e and d are omitted, and hence the notations e and d are used instead of $-e_{14}$ and $-d_{14}$, respectively, throughout this paper.)

Typical size of the sample for the dynamic mechanical measurements is 20 × 2 × 0.1 mm and the direction of the long side of the sample is parallel to the orientation axis of the fibers.

In the present work, the complex piezoelectric constants ($d = d' - id''$, i.e., the electric polarization per unit stress, and $e = e' - ie''$, i.e., the electric polarization per unit strain, in the short-circuited condition for electrodes on both surfaces of the specimen), the complex elastic constant ($c = c' + ic''$), and the complex dielectric constant ($\epsilon = \epsilon' - i \cdot \epsilon''$) were carried out at 10 Hz and at temperatures between −160°C and room temperature or 150°C.

The apparatus used to measure the piezoelectric, dielectric, and elastic constants was described elsewhere (23). The sample is vibrated by a driver activated by a.c. current through the coil. The stress and strain of the sample are detected by a load cell and a nonbonded strain gauge, respectively. The outputs of these transducers were amplified and led to an operational circuit (OC) to determine the complex elastic constant, $c = c' + ic''$. The OC is designated to automatically determine the complex response functions by using a null-balancing system which consists of a null detector, a charge amplifier, integration type-phase sensitive detectors, and sample and hold circuits. The piezoelectric charge on the short-circuited electrodes of the sample and the amplified output from the load cell or the strain gauge are both led to the OC to determine the complex piezoelectric constant $d = d' - id''$ or $e = e' - ie''$. The dielectric charge occurring on the electrodes and the applied electric voltage are also led into the OC to determine the complex dielectric constant $\epsilon = \epsilon' - i\epsilon''$.

The resolution of both real and imaginary parts of the dielectric, piezoelectric, and elastic constants are within ±0.1%. The experimental error of the four kinds of constants c, d, e, and ϵ are within ±2%.

Hydration levels were varied by equilibrating the samples at 25°C in desiccators containing different saturated salt solutions. Deionized samples of horn keratin were obtained by dialyzing them in distilled water.

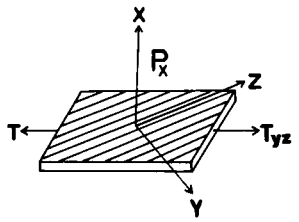

FIGURE 1 Orthogonal coordinates assigned to the specimen. Z-Axis is the orientation axis of fibers, Px is the polarization to the x-axis, and Tyz is the strain or stress in the yz plane.

RESULTS

Fig. 1 shows the orthogonal coordinates assigned to the specimen. The z-axis is the orientation axis of fibers, Px is the polarization to the x-axis, and Tyz is the strain or stress in the yz plane, respectively.

Fig. 2, *a* and *b*, shows the piezoelectric constants d' and the loss d'' of horn keratin at temperatures between −160 and 150°C at various hydration levels (21, 17, 11, 8, 5% m.c. and oven dry), respectively. With increasing temperature, d' slowly increases in the dry state and with increasing hydration, d' increases below 0°C. Particularly at 21% m.c., d' steeply decreases beyond 0°C and the temperature shifts towards higher ones with decreasing hydration. The loss d'' has large negative peaks above 0°C corresponding to the steep decrease of d' around 0°C. Hydration-dependent small loss peaks are also found at −120 and −90°C at 21% m.c., which shift towards higher temperatures with decreasing hydration. Other loss peak is found at −70°C, which is slightly hydration-dependent.

Fig. 3 shows the temperature dependence of the piezoelectric constant e' and the loss e'' of horn keratin at hydrated (21% m.c.) and dry states at temperatures between −150 and 150°C, respectively. In the dry state, e' increases from −150 to 20°C and the slope decreases beyond 20°C. In the hydrated state, e' largely increases up to 0°C and then it steeply decreases up to 50°C and e'' has loss peaks at −80, −60, and 40°C.

Fig. 4, *a* and *b*, shows temperature dependence of the elastic constants c' and the loss c'' of horn keratin with various hydration levels (21, 17, 14, 11, 8, 5% m.c. and oven dry). The constants c' decrease with increasing temperature. With increasing hydration, c' increases below −70°C and decreases above −70°C. At 21% m.c., c'' has three peaks at around −125, −110, and −70°C. The peak positions of the former two are fairly hydration

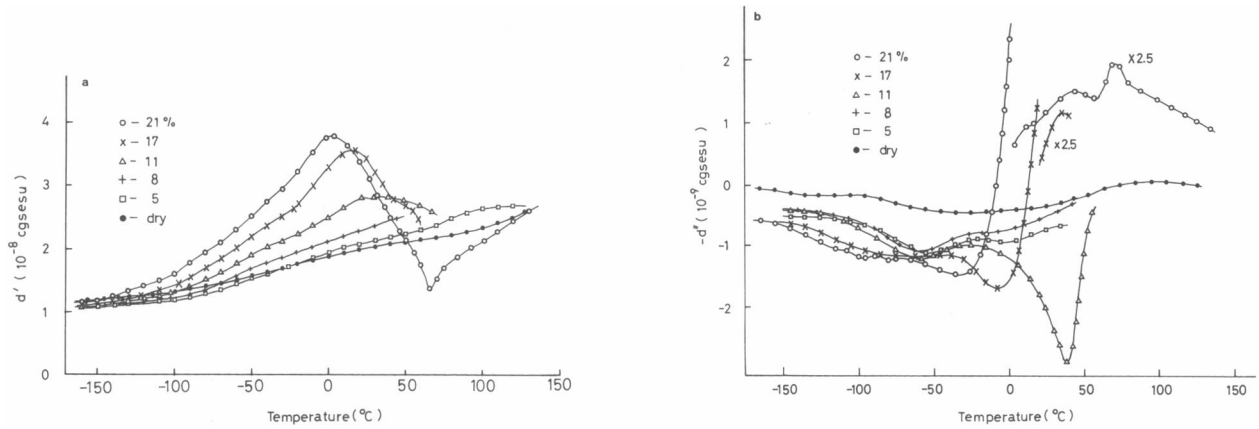

FIGURE 2 (*a*) Temperature dependence of the piezoelectric constants d' for horn keratin with hydration levels, 21, 17, 8, 5% m.c. and the dry state. (*b*) Temperature dependence of the piezoelectric losses d'' for horn keratin corresponding to the hydration levels in *a*.

dependent and the latter seems to be slightly hydration dependent.

Fig. 5, *a* and *b*, shows the dielectric constants ϵ' and the loss ϵ'' of horn keratin with various hydration levels (21, 17, 14, 11, 8, 5% m.c. and oven dry) at temperatures between -150 and 50°C. The constants ϵ' and ϵ'' increases with hydration levels. The loss ϵ'' has a peak at about -125°C at 21% m.c., which shift up to -30°C with decreasing hydration. Two other loss peaks are found at -100 and -70°C. The former is fairly hydration-dependent and the latter is slightly hydration-dependent.

Fig. 6 shows hydration dependence of the elastic, dielectric and piezoelectric loss peaks appeared at around -120°C. The curves of these three kinds of loss peak almost agree well with each other and they have three regimes, 0–2.5% m.c. (regime I), 2.5–20% m.c. (regime II), and >20% m.c. (regime III).

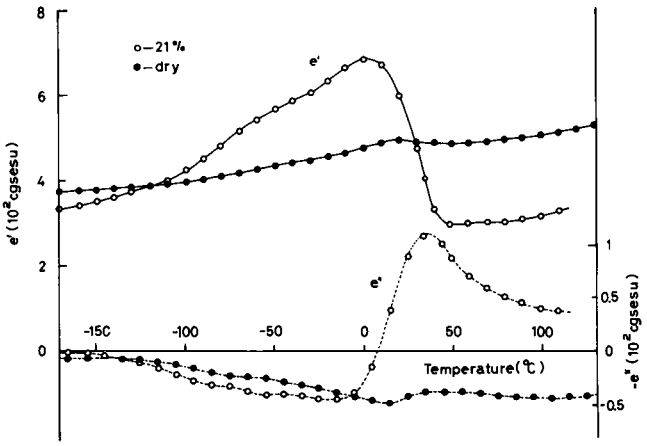

FIGURE 3 Temperature dependence of the piezoelectric constants e' and e'' for horn keratin with hydration levels, 21% m.c. and the dry state.

Fig. 7 shows the hydration dependence of c' of horn keratin. The constant c' at 0°C hardly depends on hydration between 0 and 4% m.c. and decreased at hydrations >4% m.c. On the other hand, c' at -150°C increases with increasing hydration.

Fig. 8 shows the hydration dependence of d' of horn keratin at -150°C. The curve has a deflection point at ~3.4% m.c. Below 3.4% m.c., d' decreases and above 3.4% m.c., d' increases with increasing hydration levels.

DISCUSSION

Piezoelectric models of keratin

We will consider possible models of keratin structure from the piezoelectric measurements. Feughelman (17) first proposed a two-phase model from the mechanical measurements, which consists of parallel microfibrils and a matrix region surrounding them. We first adopt a piezoelectric two-phase model similar to the Feughelman's mechanical model, which consists of a piezoelectric phase (c; mainly the microfibrils) and a nonpiezoelectric phase (m; mainly the matrix region) connected in parallel as shown in Fig. 9 *A*. (In the piezoelectric model, not only the mechanical properties but also the dielectric and piezoelectric properties are introduced.) For Fig. 9 *A*, the piezoelectric constants, e and d, are easily formulated as follows (24).

$$e = \phi_c e_c \cdot \frac{\epsilon_m}{\phi_c \epsilon_m + \phi_m \epsilon_c} \tag{1}$$

$$d = \phi_c e_c \cdot \frac{1}{\phi_m c_m + \phi_d c_c} \cdot \frac{\epsilon_m}{\phi_c \epsilon_m + \phi_m \epsilon_c}, \tag{2}$$

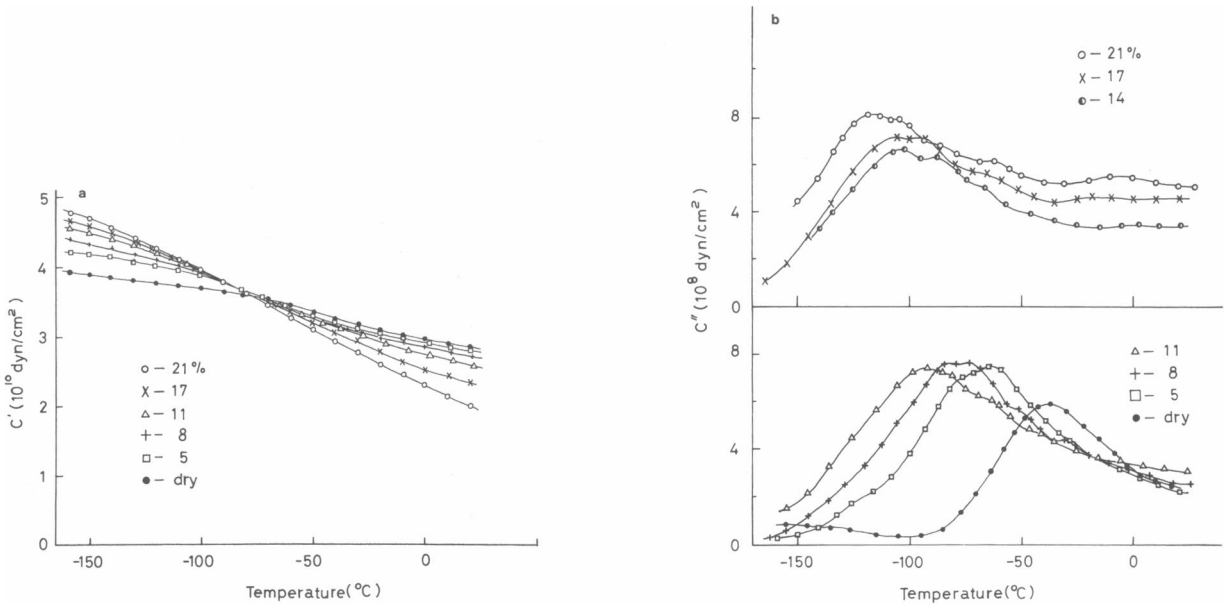

FIGURE 4 (*a*) Temperature dependence of the elastic constants c' for horn keratin with hydration, 21, 17, 11, 8, 5% m.c. and the dry state. (*b*) Temperature dependence of the elastic losses c'' for horn keratin with hydration, 21, 17, 14, 11, 8, 5% m.c. and the dry state.

where $\phi_m = l_m/(l_m + l_c)$, $\phi_c = l_c/(l_m + l_c)$, l_m and l_c are the thickness of the nonpiezoelectric and piezoelectric phases, respectively, e_c is the polarization per unit strain of the piezoelectric phase alone, and ϵ and c are the dielectric and elastic constants in the respective phases denoted by the subscripts m and c. Further, the dielectric constants for Fig. 9 *A* can be easily formulated as follows.

$$\epsilon = \frac{\epsilon_m \epsilon_c}{\phi_c \epsilon_m + \phi_m \epsilon_c}. \tag{3}$$

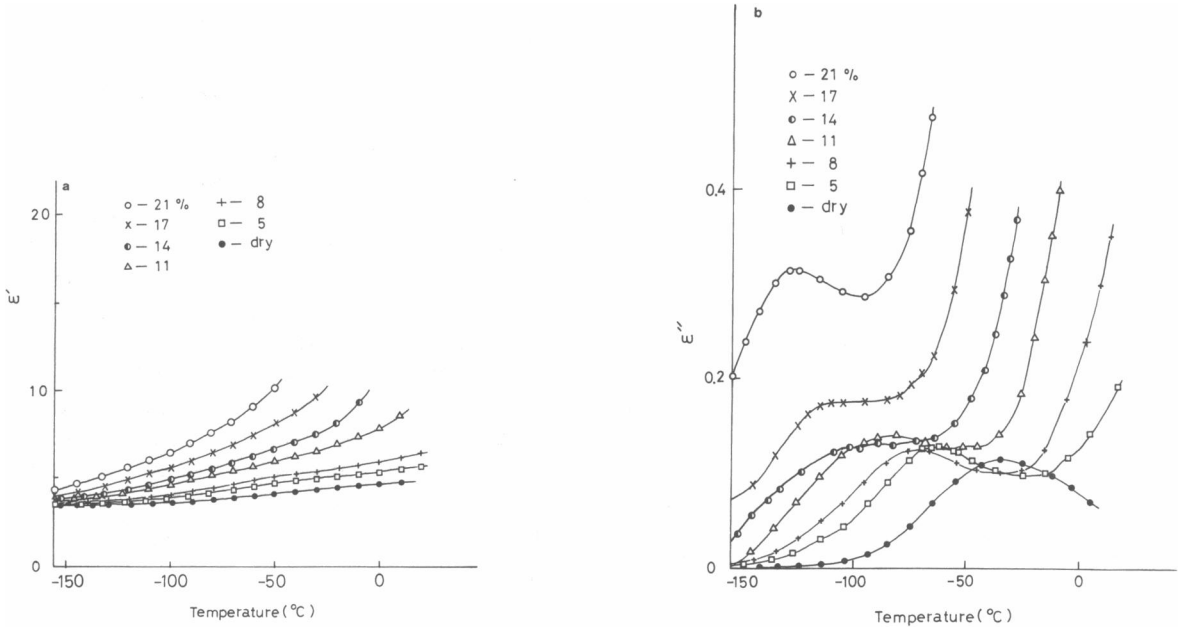

FIGURE 5 (*a*) Temperature dependence of the dielectric constants ϵ' with hydration levels, 21, 17, 14, 11, 8, 5% m.c. and the dry state. (*b*) Temperature dependence of the dielectric losses ϵ'' for horn keratin corresponding to the hydration levels in *a*.

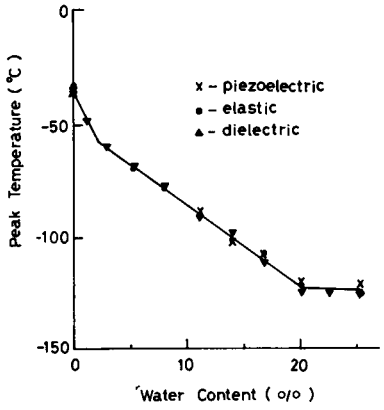

FIGURE 6 Hydration dependence of the piezoelectric, dielectric, and elastic loss peaks around −120°C for horn keratin.

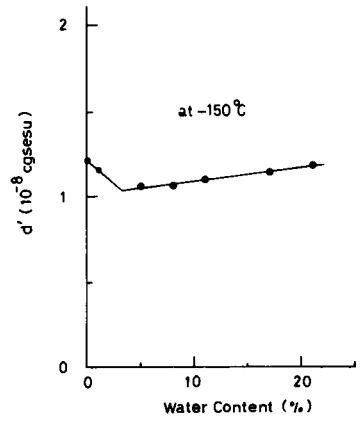

FIGURE 8 Hydration dependence of the piezoelectric constants d' at −150°C for horn keratin.

By substituting Eq. 3 into Eq. 1, we obtain

$$e = \phi_c e_c \epsilon / \epsilon_c. \tag{4}$$

If we assume e_c and ϕ_c little depend on temperature as expected as the property of crystalline parts, we get the following equation from Eq. 4.

$$\tilde{e}/e_0 = \tilde{\epsilon}/\epsilon_0, \tag{4'}$$

where $\tilde{e}$ and e_0 are the piezoelectric constants at any temperatures T_1 and T_2, respectively, and $\tilde{\epsilon}$ and ϵ_0 are the dielectric constants at T_1 and T_2, respectively.

Experimentally, if $T_1 = -150$°C and $T_2 = 0$°C, we obtain $\tilde{e}/e_0 \sim 1.3$ from Fig. 3 and $\tilde{\epsilon}/\epsilon_0 \sim 1.4$ from Fig. 5 at dry state. These values agree well with each other as expected from Eq. 4'. Thus, Fig. 9 *A* appears good for the keratin structure. On the other hand, as the elastic constant c of Fig. 9 *A* is written as follows.

$$c = \phi_m c_m + \phi_c c_c, \tag{5}$$

and hence the piezoelectric constant d is rewritten from Eqs. 2, 3, and 5 as follows.

$$d = \phi_c e_c \epsilon / \epsilon_c c. \tag{6}$$

Using Eq. 6 under the assumption that e_c and ϕ_c depend little on temperature already mentioned, we obtain

$$\tilde{d}/d_0 = \tilde{\epsilon} c_0 / \epsilon_0 \tilde{c}, \tag{7}$$

where $\tilde{d}$ and d_0 are the piezoelectric constants at temperatures T_1 and T_2, respectively, and $\tilde{c}$ and c_0 are the elastic constants at T_1 and T_2, respectively. If $T_1 = -150$ and $T_2 = 0$°C, we obtain $\tilde{d}/d_0 \sim 1.7$ by substituting the values of $\tilde{\epsilon}/\epsilon_0 \sim 1.4$ and $\tilde{c}/c_0 \sim 1.2$ (at dry state from Fig. 4 *a*)

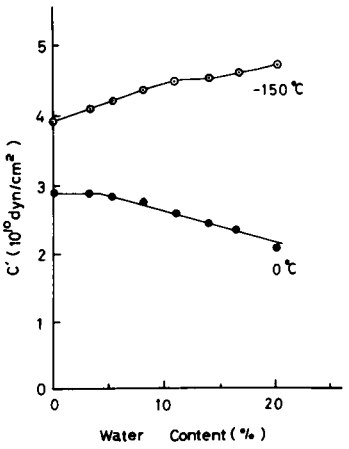

FIGURE 7 Hydration dependence of the elastic constants c' at −150 and 0°C, respectively, for horn keratin.

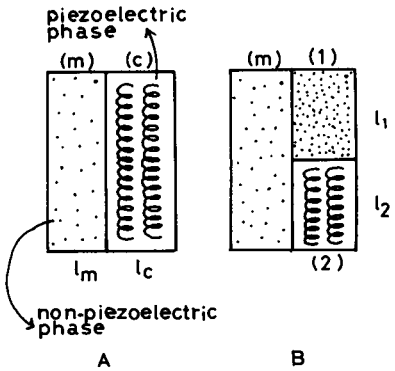

FIGURE 9 Piezoelectric models of the keratin structure. (*A*) *m*, nonpiezoelectric phase; *c*, piezoelectric phase. (*B*) Phases 1 and 2 are nonpiezoelectric and piezoelectric, respectively. The size of the respective phases is denoted by *l* with subscripts m, c, 1, and 2.

into Eq. 7. On the other hand, we experimentally obtain $\tilde{d}/d_0 \sim 1.6$ at dry state from Fig. 2 *a*. These values of $\tilde{d}/d_0$ agree well with each other. Thus, model A is indicated to be good for the keratin structure again.

On the other hand, at dry state the decrease of the slope of e above 20°C as shown in Fig. 3 cannot be explained by Fig. 9 *A*. To understand the behavior, as is described below we have only to introduce such a model that the piezoelectric phase has elastically different two parts connected in series, one is piezoelectric and the other is nonpiezoelectric. This model is shown in Fig. 9 *B* and is found to be similar to a mechanical series zone model proposed by Feughelman et al. (18). For Fig. 9 *B*, the piezoelectric constant e is formulated as follows.

$$e = e_2 \cdot \frac{\phi_2 c_1}{\phi_2 c_1 + \phi_1 c_2} \cdot \frac{\phi_c \epsilon_m}{\phi_c \epsilon_m + \phi_1 \phi_m \epsilon_1 + \phi_2 \phi_m \epsilon_2}, \qquad (8)$$

where the subscripts 1 and 2 refer to the nonpiezoelectric phase and the piezoelectric phase, respectively, $\phi_1 = l_1/(l_1 + l_2)$, $\phi_2 = l_2/(l_1 + l_2)$, and l is the length of the respective phases. By using Eq. 8, we can suggest that the larger decrease of c_1 than that of c_2 against temperature causes the decrease of the slope of e' above 20°C.

Thus, by introducing two serially connected zones with the different elastic constants (one is piezoelectric and the other is nonpiezoelectric) into the microfibrils, more exact keratin model can be obtained.

Actions of bound water in keratin

Keratin appears to have three regimes in the hydration of water. Fig. 6 shows the hydration dependence of the piezoelectric, dielectric, and elastic loss peaks, which shift between −120 and −30°C. The curves of these three peaks agree well with each other. This fact implies that the relaxing units are pretty localized and thus the units are probably related to tightly bound water in keratin. (We already found the similar hydration-dependent loss peaks for collagen at −120°C) (25). Further, the curves can be divided into three regimes in hydration of water: (a) hydration levels <2.5% m.c., (*b*) 2.5–20% m.c., and (*c*) >20% m.c. These three regimes are also found in the curves of Young's modulus vs. hydration for wool fibers by Speakman (10), which has deflection points at 6 and 21% m.c. Algie and Gamble (7) also found deflection points at 2% m.c. in a curve of a dielectric absorption against hydration and at 23% m.c. in the curves d.c. conductance and dielectric absorption against hydration for horn and wool. We also found a deflection point in the curve of the hydration dependence of the elastic constant c at 0°C (Fig. 1) and the piezoelectric constant d at −150°C (Fig. 8).

We found a viscoelastic transition due to adsorbed water in the keratin structure at around −70°C. As seen in Fig. 4 *a*, actions of water are clearly different below and above −70°C. (Similar behavior is also found in Youngs modulus of wool fibers by Druhala and Feughelman [11].) For example, the elastic constant at −150°C increases with increasing hydration, whereas that at 0°C hardly changes <4% m.c. and decreases >4% m.c. (Fig. 7). Thus, the viscoelastic transition of the keratin structure seems to be due to regime *b* water.

Water in regime *a* is considered to form water-bridges between polar sites of polypeptide chains by hydrogen bonding so as to increase the elastic constant. On the other hand, water in regime *b* is considered to adsorb between the polar groups in the side chains as described below. We recently observed that after the side chains of poly(γ-methyl-L-glutamate) are made more hydrophilic with ethylene diamine, the viscoelastic transition appears at around −20°C in its elastic constants (Maeda and Ebihara, submitted for publication). On the other hand, we found only the increase of the elastic constant due to water for poly(*N*-isopropylacrylamide) or PNIPAM below 0°C (26). This behavior may be attributed to the less hydrophilic groups in its side chains as well as PMLG. Thus, water molecules, particularly in regime *b*, are thought to loosely adsorb around the respective ionic groups of the side chains to weaken the intermolecular coulombic interaction above −70°C. The water molecules in regime *b*, however, may have some bound states, according to the results of NMR spectroscopic studies for hydrated wool by Lynch and Marsden (14, 15).

Adsorption regions of water in keratin

We consider that the information about the adsorption sites of water in keratin can be obtained from hydration and temperature dependence of e and d.

At 21% m.c., d' and e' decrease above 0°C with increasing temperature. (The steep decrease of d' was also found at −50°C for collagen [25] and wood [27].) Such decrease of d' and e' is considered to be mainly attributed to interfacial and electrode polarization which may be induced by the mobile ions contained in keratin. Algie (7) demonstrated the ϵ'' for keratin at low frequencies can be decomposed of an d.c. conduction and an interfacial polarization. (For collagen, ϵ'' increases with decreasing frequency, seemingly due to an interfacial polarization [29]. To understand the ionic effects on e and d (28, 30), they must be extended to include the electric conduction in them. For this purpose, the dielectric constant in Eq. 1 must be replaced by $\epsilon^* = \epsilon' - i4\pi\sigma/\omega$,

where ω is angular frequency and σ is electric conductivity. Thus, e is rewritten as follows (13, 31, 32).

$$e = \phi_c e_c \cdot \frac{\epsilon_m^*}{\phi_c \epsilon_m^* + \phi_m \epsilon_c^*}. \quad (9)$$

When the electrode polarization is effective (33), Eq. 8 is multiplied by $\epsilon_\ell^*/(\epsilon_\ell^* + \epsilon_s^*)$, where ϵ_ℓ^* is a capacitance which expresses a polarization near the electrode defined as $\epsilon_\ell^* = \epsilon_\ell\ (i\omega)^{n-1}$ $(0 \leqq n \leqq 1)$ and ϵ_s^* is the dielectric constant defined in Eq. 3 (34). This term cannot be neglected, as ϵ_s^* becomes larger with hydration. If such electrode polarization is ineffective, the real part of Eq. 9 is written as follows.

$$\theta' = \phi_c e_c \cdot \frac{\omega^2 \epsilon_m(\phi_c \epsilon_m' + \phi_m \epsilon_c') + 16\pi^2 \sigma_m(\phi_c \sigma_m + \phi_m \sigma_c)}{\omega^2(\phi_c \epsilon_m' + \phi_m \epsilon_c')^2 + 16\pi^2(\phi_c \sigma_m + \phi_m \sigma_c)^2}. \quad (10)$$

Eq. 10 shows that the increase of σ_m and ϵ_m' with temperature rises e' and the increase of ϵ_c' and σ_c can reduce e'. (The same is true of d'.) The conductivity σ_c is considered to be a linear combination of the conductivity in the surface of the piezoelectric phase and the bulk conductivity of the piezoelectric phase (35). The surface conductivity indicates that water molecules may form thin conductive layers with ions trapped just around the microfibrils. The increase of the surface conductivity causes interfacial polarization (Maxwell-Wagner effect) to increase ϵ' and ϵ'' and to decrease d' and e'. On the other hand, as the electric conduction of the sample, hence ϵ_s, increases with temperature, the electrode polarization would become effective to decrease d' and e'.

In summary, we suppose water molecules appear to at least adsorb in the amorphous matrix region and just around the microfibrils. In the amorphous matrix region, water molecules in regime *b* appear to induce the increase of the electric conductivity σ_m and the increase of the mobilities of portions of the peptide chains (that is, the increase of ϵ_m' and the decrease of c_m) to result in the increase of d' and e' and the decrease of c'. Water molecules, particularly in regime *c*, would adsorb just around the microfibrils, where they are associated with each other to form conductive layers with trapped ions (Haly and Snaith [36, 37] actually reported a clustering of water 23% m.c. in hydrated wool by measuring its specific heat). The mobility of the ions trapped in the layers increases with increasing temperature to induce an interfacial polarization and hence the piezoelectric polarization of the crystalline α-helices of the microfibrils is reduced by the ions. However, the mobile ions in the amorphous matrix region, some of which would be released from the layers by the regime *c* water, also seem to induce electrode polarization and hence decrease the piezoelectric polarization. Such behavior of the piezoelectric constant can be seen beyond 0°C.

Received for publication 20 December 1988 and in final form 16 June 1989.

REFERENCES

1. Fraser, R. D. B., T. P. MacRae, and E. Suzuki, 1976. Structure of keratin microfibril. *J. Mol. Biol.* 108:435–452.
2. Fraser, R. D. B., T. P. MacRae, G. R. Millward, D. A. D. Parry, E. Suzuki, and P. A. Tulloch. 1971. The molecular structure of keratins. *Appl. Polym. Symp.* 18:65–83.
3. Fraser, R. D. B., and T. P. MacRae. 1973. The structure of keratin. *Polymer.* 14:61–67.
4. Fraser, R. D. B., and G. E. Rogers. 1972. Keratins: Their Composition, Structure, and Biosynthesis. Charles C. Thomas, Springfield, IL. p. 111.
5. King, D. 1947. Electric polarisation in keratin-water and keratin-methyl alcohol systems. *Trans. Faraday Soc.* 43:601–611.
6. Algie, J. E. 1969. Some dielectric properties of wool. *Kolloid-z. und Zeitschrift für Polymere.* 234:1069–1078.
7. Algie, J. E., and R. A. Gamble. 1973. Dielectric properties of wool and horn containing absorbed water. *Kolloid-z. und Zeitschrift für Polymere.* 251:554–562.
8. Algie, J. E. 1964. Dielectric constant and conductance changes in wool fibers produced by step changes in the relative humidity. *Text. Res. J.* 34:477–486.
9. Algie, J. E., and I. C. Watt. 1965. The effect of changes in the relative humidity on the electrical conductivity of wool fibers. *Text. Res. J.* 35:922–929.
10. Speakman, J. B. 1929. The rigidity of wool and its change with adsorption of water vapour. *Trans. Faraday Soc.* 21:92–103.
11. Druhala, M., and M. Feughelman. 1971. Mechanical properties of keratin fibres between −196°C and 20°C. *Kolloid-z. und Zeitschrift für Polymere.* 248:1032–1033.
12. Menefee, E., and G. Yee. 1965. Thermally-induced structural changes in wool. *Text. Res. J.* 35:801–812.
13. Fukada, E. 1974. Piezoelectric properties of biological macromolecules. *Adv. Biophys.* 6:121–155.
14. Lynch, L. J., and K. H. Marsden. 1966. Study of the wool-water system by means of pulsed nuclear-magnetic-resonance techniques. *J. Text. Inst. Trans.* 57:T1–T7.
15. Lynch, L. J., and K. H. Marsden. 1969. NMR of absorbed system. II. A NMR study of keratin hydration. *J. Chem. Phys.* 51:5681–5691.
16. Feughelman, M. and A. R. Haly. 1962. The physical properties of wool fibers at various regains. *Text. Res. J.* 32:966–971.
17. Feughelman, M. 1959. A two-phase structure for keratin fibers. *Text. Res. J.* 29:223–228.
18. Feughelman, M., and A. R. Haly. 1960. The mechanical properties of wool keratin and its molecular configuration. *Kolloid-z. und Zeitschrift für Polymere.* 168:107–115.
19. Feughelman, M. 1980. Basic wool physics. *Proc. Int. Wool Text Res. Conf.* 6:35–57.

20. Heideman, G., and H. Halboth. 1970. The fibrillar swelling of keratin. *Text. Res. J.* 40:861–862.

21. Spei, M., and H. Zahn. 1979. X-Ray small-angle examination of swollen fibre keratins. *Melliland Textilberichte.* 60:523–525.

22. Spei, M. 1985. Sorption behaviour and thermal stability of the microfibril-matrix-complex of keratin. *Proc. Int. Wool Text. Res. Conf.* 7:312–318.

23. Furukawa, T., and E. Fukada. 1976. Piezoelectric relaxation in poly(γ-benzyl-glutamate). *J. Polym. Sci.* 14:1979–2010.

24. Maeda, H., and E. Fukada. 1976. The dependence on temperature and hydration of piezoelectric and elastic constants of bone. *Jpn. J. Appl. Polym. Phys.* 15:2333–2336.

25. Maeda, H., and E. Fukada. 1982. Effect of water on piezoelectric, dielectric, and elastic properties of bone. *Biopolymers.* 21:2055–2068.

26. Maeda, H., S. Ito, H. Yamamoto, and M. Suda. 1986. Adsorption of thermoreversible polymers on silica. *Bull. Res. Inst. Polym. Text.*144:29–34.

27. Maeda, H., and E. Fukada. 1987. Effect of bound water on piezoelectric, dielectric, and elastic properties of wood. *J. Appl. Polym. Sci.* 33:1187–1198.

28. Maeda, H., and E. Fukada. 1981. Temperature and hydration dependence of piezoelectric constant of tendon with various amount of ions. Rept. Progr. Polym. Phys. Japan. XXI:617–620.

29. Sasaki, N. 1984. Dielectric properties of slightly hydrated collagen: time-water content superposition analysis. *Biopolymers.* 23:1725–1734.

30. Maeda, H. & E. Fukada, 1981. Temperature and hydration dependence of piezoelectric constant of bamboo with various amount of ions. *Rep. Progr. Polym. Phys. Jpn.* 21:333–336.

31. Fukada, E., and M. Date. 1970. Mechanical and electrical models for piezoelectric dispersions in oriented polymers. *Polym. J.* 1:410–417.

32. Date, M. 1973. The influence of d.c. conductivity on piezoelectric constants of polymers: a spherical dispersion model. *Rep. Progr. Polym. Phys. Jpn.* 16:473–476.

33. Furukawa, T., K. Ishida, and E. Fukada. 1979. Piezoelectric properties in the composite systems of polymers and PZT ceramics. *J. Appl. Phys.* 50:4904–4912.

34. Johnson, J. F., and R. H. Cole. Dielectric polarization of liquid and solid formic acid. *J. Am. Chem. Soc.* 73:4536–4540.

35. Ueda, H., and E. Fukada. 1975. Piezoelectric relaxation in a dispersed system of PZT-ceramics powders in polyvinyl alcohol. *Rep. Progr. Polym. Phys. Jpn.* 18:367–370.

36. Haly, A. R., and J. W. Snaith. 1961. Specific heat studies of various wool-water systems. *Biopolymers.* 6:1355–1377.

37. Haly, A. R. 1969. The specific heat of wool containing an additive and the heat of fusion of the absorbed water. *J. Text. Inst.* 60:403–410.